Doklady Earth Sciences, Vol. 397, No. 5, 2004, pp. 663–667. Translated from Doklady Akademii Nauk, Vol. 396, No. 5, 2004, pp. 686–690.

GEOGRAPHY

Evidence for the Leading Role of Temperature Variations Relative to Greenhouse Gas Concentration Variations in the Vostok Ice Core Record

N. V. Vakulenko, Academician of the RAS V. M. Kotlyakov, Academician of the RAS A. S. Monin, and D. M. Sonechkin

Received March 3, 2004

The cause-and-effect interrelation between long-term variations in temperature and greenhouse gas concentration (GGC) in the atmosphere is an important aspect of the problem of climatic variations. According to [1], anthropogenic GGC growth is of primary significance, whereas recent warming is a consequence of the GGC-induced greenhouse effect [1]. However, the available paleoclimatic data cast doubt on the unconditional unidirectional character of this interrelation. It has been established that the onset of the four glacial epochs was characterized by synchronous (coherent) decreases of the air temperature (based on the deuterium content *d*D in the Vostok ice core) and the methane (M) concentration, while the carbon dioxide (C) concentration decreased with a small lag [2]. The onset of the interglacial warm epoch was probably triggered by insolation growth. The increase of GGC (particularly, M) was at first slow and then significantly rapid. According to [3], the C growth lag was 600 ± 200 yr, which is within the relative accuracy range of time scales for the compared series (approximately ±1000 yr), because air bubbles, which are used for the GGC assessment, diffuse within the ice core for several thousands of years after snow deposition. In [4], air bubbles enclosed in the Vostok ice core were analyzed with a resolution of 100 yr for the interval of 230–250 ka BP, (approximately corresponding to Warm Period III). The temperature and GGC variations were estimated using δ^{40}Ar concentrations within the same bubbles. Thus, the combined inaccuracy of time scales for the studied series was minimized. On the whole, the temperature variations turned out to be 800 ± 200 yr ahead of the GGC variations. However, the authors of [4] do not explain why δ^{40}Ar variations can be likened to air temperature variations. It is also unclear why temporal relationships between the temperature and GGC can differ at different time scales and during different phases of the glacial cycle, as has been shown by some model calculations [5].

Shirshov Institute of Oceanology, Russian Academy of Sciences, Nakhimovskii pr. 36, Moscow, 117851 Russia; e-mail: dsonech@rhmc.mecom.ru
Institute of Geography, Russian Academy of Sciences, Moscow, Russia
Hydrometeorological Center of Russia, Moscow, Russia

The aim of this work is to quantitatively check the conclusions in [2–4] by calculating cross correlations of the average temperature (based on the deuterium *d*D content) and GGC variations estimated for all glacial cycles in the Vostok ice core. The cross correlations were specified for time scales of *d*D and GGC variations and phases of the glacial cycle using the technique of wavelet transform (WT) of the time series

$$W(b, a) = a^{-1/2}\int T(t)G((t-b)/a)dt, \qquad (1)$$

where $T(t)$ is the analyzed series and $G((t-b)/a)$ are functions obtained by various shifts (b) and rescaling (a) of a single specially selected wavelet function $G(t)$.

It appeared that all four warm periods in the Vostok core record in fact began with the temperature growth. This is true, at least, of the long-period fluctuations that determine the main cycle of glacial and interglacial epoch alternations. Both the beginning and termination of GGC growth always demonstrated a lag relative to the warming–cooling replacement episode. The estimated lag of 2–3 ka is greater than the combined inaccuracy of the time scale series. Thus, GGC variations followed rather than anticipated temperature variations during the critical episodes of the glacial cycle.

The calculation procedure was as follows. Series *d*D, C, and M were preliminarily centered and normalized (their average values and dispersions became equal to zero and unity, respectively) so that the series trends could formally be compared.

In order to define local (in time and scale) trends, we used the wavelet function (the first Gaussian derivative)

$$G\left(\frac{t-b}{a}\right) = \frac{1}{\sqrt{\Gamma(1.5)}}\frac{d}{dt}\exp\left\{-0.5\left(\frac{t-b}{a}\right)^2\right\}, \qquad (2)$$

where $\Gamma(\cdot)$ is the gamma function. The wavelet scale of the function (2) is five times as great as the Fourier scale. Consequently, variations of trends $W(b, a)$ at the minimal scale a = 1 ka calculated on the basis of

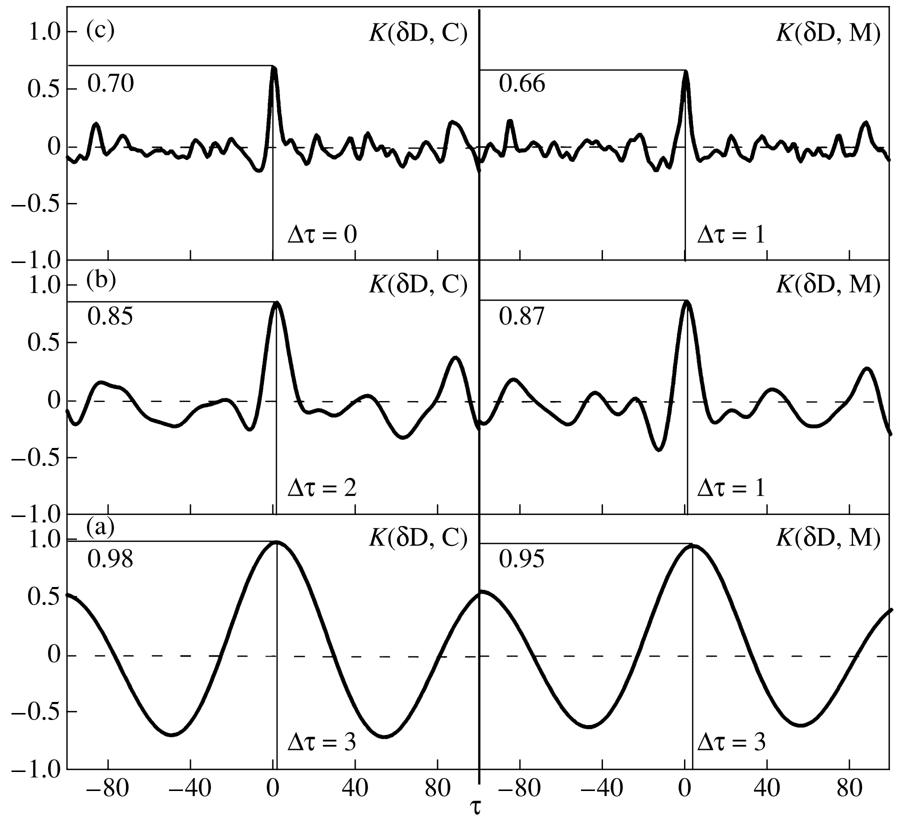

Fig. 1. Temporal cross correlation of the deuterium (δD) series with carbon dioxide (C) and methane (M) series at the scale of (a) 100, (b) 20, and (c) 5 ka. Numbers indicate maximum values of cross correlations and time lags (in ka) when these cross correlations are observed.

Eqs. (1) and (2) correspond to successive five-point series intervals with a resolution of 1 ka.

Cross correlations were first calculated for the whole series length:

$$K(\delta\mathrm{D}, i)_{\delta\tau} = \Delta^{-1}\int_{\Delta} W(b, a)_{d\mathrm{D}} W(b + \delta\tau, a)_i db, \quad (3)$$
$$\delta\tau = 0, \pm 1, \pm 2, \ldots, \quad i = \mathrm{C}, \mathrm{M},$$

where Δ is the length of the considered series for $a = 20$, 4, and 1 ka, which correspond to trend scales of 100, 20, and 5 ka, respectively (Fig. 1). It appeared that cross correlation maxima of $K(\delta\mathrm{D}, i)_{\delta\tau} = 0.98$ and 0.95 are observed for C and M, respectively, at the scale of 100 ka if the shift $\delta\tau = +3$; i.e., the temperature trend is 3 ka ahead of the GGC trend. This value exceeds the combined inaccuracy of the time scales. At the scale of 20 ka, this lag is at significance limit (2.1 and 1 ka) and cross-correlation maxima are even lower (0.85 and 0.87). At the scale of 5 ka, the time lag slightly differs from zero and the cross-correlation maxima are lower (0.70 and 0.66).

Cross correlations were then considered for particular phases of the glacial cycle using paired products of WT results on the plane (b, a):

$$\eta W(b, a) = W(b, a)_{d\mathrm{D}} W(b, a)_i, \quad i \equiv \mathrm{C} \text{ or } \mathrm{M}. \quad (4)$$

If $\eta W(b, a) > 0$, the particular time scale (a) and the particular phase (b) of the glacial cycle were characterized either by simultaneous warming and GGC growth or simultaneous cooling and GGC decrease. If $\eta W(b, a) < 0$, warming was accompanied by GGC reduction or the cooling was synchronous with GGC growth. Figure 2 shows the plot $\eta W(b, a)$ for the pair dD/C. The plot for the pair dD/M is almost identical and, therefore, is omitted from consideration. The right part of Fig. 2 shows the plot of average values

$$\mathrm{MUL}(a) = \Delta^{-1}\int_{\Delta} \eta W(b, a) db. \quad (5)$$

All average values are positive and increase with the scale growth. Hence, local trends dD and C are generally coherent in time. This confirms the results of cross-correlation analysis after [3]. Figure 2 also shows the time variations of $\eta W(b, a)$ at the scale of 5 ka with positive delta-shaped surges occurring approximately during each of the warm epochs. In other periods, the values are negative; i.e., variations in dD and C were low and incoherent during cold epochs. As is evident from the whole record, at larger scales (>40 ka), positive

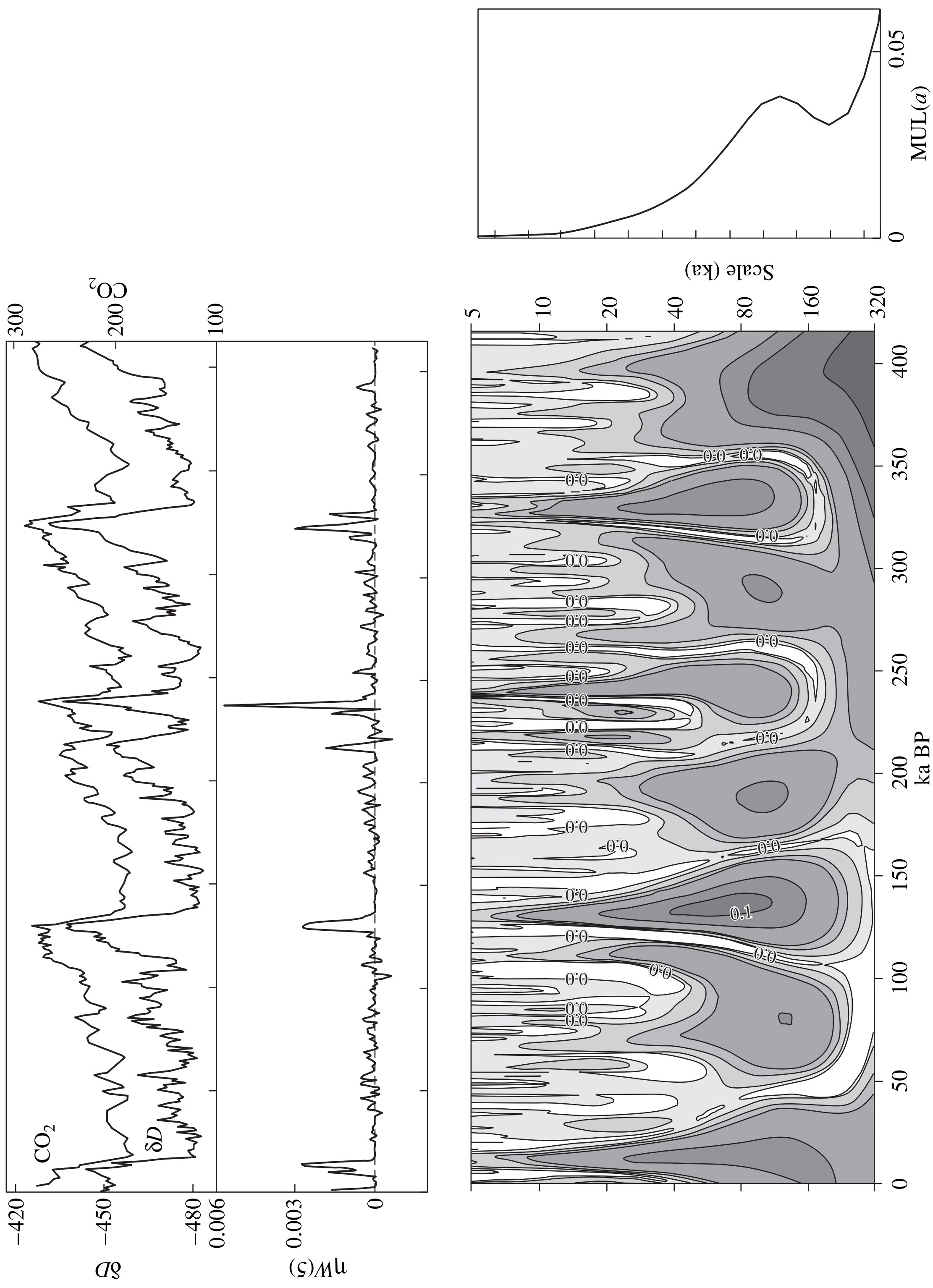

Fig. 2. The time–time scale plot demonstrating products of the wavelet transform of δD and C series (shown in the upper part). The plot in the middle shows these products at the scale of 5 ka. The plot to the right shows the average (in time) product as a function of the scale.

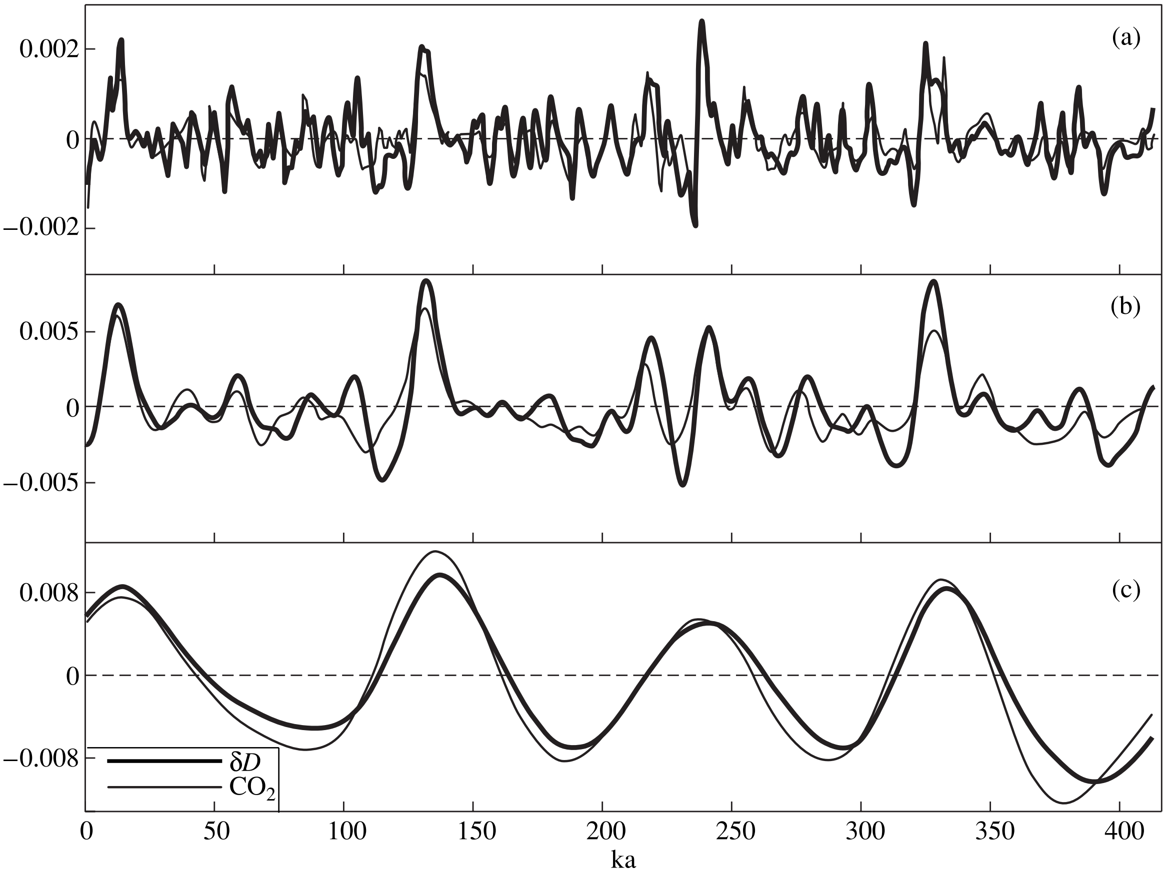

Fig. 3. Temporal plots for wavelet transforms of deuterium and carbon dioxide series at scales of (a) 5, (b) 20, and (c) 100 ka. Positive values correspond to local warming trends (growth of carbon dioxide concentrations); negative values, to cooling trends (decrease in carbon dioxide concentrations). The moments of transition from warming (increase of C) to cooling (decrease of C) correspond to the points where the δD plot crosses the zero ordinate from the top to bottom. The moments of reversed transition (termination of maximal cooling, in particular) correspond to the points where the δD plot crosses the zero ordinate from the bottom to top.

surges $\eta W(b, a)$ become even more powerful and—which is more important—longer as compared with the combined inaccuracy of the time scales of the compared series. They resemble pairs of "drops" falling from small time scales onto large ones during warm periods. In contrast, negative areas in large-scale intervals resemble narrow "ribbons" enveloping the drops. The right drop in each pair corresponds to synchronous warming and GGC growth, whereas the left one corresponds to cooling and GGC decrease. The presence of drops can be interpreted as a sign of the self-similarity of climatic fluctuations, because local trends of series are coherent within the drop regardless of the time scale. The bifurcation of ribbons in small-scale intervals (<40 ka) reflects the mostly incoherent warming/cooling episodes and GGC variations of lower orders. The self-similarity of these small scales allows us to exclude them from consideration and restrict ourselves to analysis of trends in large-scale intervals, for which combined inaccuracies of time scales are insignificant.

Figure 3 shows the WT (1) plots of *d*D and C series for time scales of 5, 20, and 100 ka (the M plot is similar to that for C and, therefore, omitted from consideration). Comparison of the most simple (in terms of structure) and reliable (in terms of the inaccuracy of time scale) plots for the 100 ka scale and analysis of plots compiled for lower scales show that relations between local *d*D and GGC trends changed uniformly during all four glacial cycles. At the beginning of warming, the *d*D plot crossed the zero value from bottom to top. In the complete plot of $\eta W(b, a)$ in Fig. 2, such moments correspond to the right edges of ribbons with negative values. The GGC trends became positive only several thousand years later and, then, turned out to be stronger than the *d*D trend. This is evident from intersections of *d*D and C plots with each other at the moments preceding the maximal phases of the *d*D plot. Subsequently, the warming trend slowed down and gave way to the cooling trend. This is reflected in the intersection of the zero ordinate by the *d*D plot from top to bottom in Fig. 2 and the intersection of negative values of $\eta W(b, a)$ at the scale of 100 ka by ribbons in Fig. 3.

The GGC values continued to increase for some time, as is evident from the preservation of their trends above the zero ordinate. Then, they also began to decrease, leaving behind the *d*D trend. Such a scenario was retained up to the maximal glaciation stages that terminated the glacial cycles. These results qualitatively correspond to those presented in [2]. Moreover, they are stable, relative to the inaccuracies of the time scales of the series.

At the scale of <40 ka, this succession of relations between local trends takes place over a shorter period and is repeated several times during the main 100-ka-long glacial cycle. One can see distortions in these interrelations at the scale of 20 ka. For instance, warming stages II and IV were likely triggered by C growth approximately 150 and 350 ka BP, respectively. It is difficult to estimate whether this interrelation is real or caused by inaccuracies in data and their scales. If the moments, after which *d*D values monotonously increased up to the warming maximum (approximately 140 and 335 ka BP, respectively), are considered starting points of these warming events, then the leading role belongs to the temperature.

Thus, one can conclude that temperature variations always preceded GGC variations during the four main glacial cycles recorded in the Vostok ice core. Of particular importance is the fact that the temperature began to decrease after reaching a very high value, although the GGC values continued to increase. Will we witness cooling in the near future, even though anthropogenic GGC will continue to increase?

ACKNOWLEDGMENTS

This work was supported by the Russian Foundation for Basic Research, project no. 02-05-64229.

REFERENCES

1. *Intergovernmental Panel on Climate Change. Climate Change 2001. The Scientific Basis. Contribution of Working Group I to the Third Assessment Rept. of IPCC*, Ed. by J. T. Houghton, L. G. Meira-Filha, and B. A. Callander (Cambridge, 2001).
2. J. R. Petit, J. Jouzel, D. Raynaud, *et al.*, Nature **399**, 429 (1999).
3. Y. Fischer, M. Wahlen, J. Smith, *et al.*, Science **283**, 1712 (1999).
4. N. Caillon, J. P. Severinghaus, J, Jouzel, *et al.*, Science **299**, 1728 (2003).
5. H. Gildor and M. Ghil, Geophys. Res. Lett. **29**, 11-1 (2002).